CA-3 | 29

ASAT

MILITARY TECHNICAL COLLEGE
CAIRO - EGYPT

A TURBULENCE MODEL FOR WIND FLOWS ABOVE FIRE AREAS

SAMIR S. AYAD*

ABSTRACT

The object of the present work is to model the wind flow field above fire areas. A cylinderical domain of height H and radius Ro is considered with a concentric fire area of radius Rf at its bottom. The rate of heat flux within the fire radius $\dot{Q}''$ is specified.

Averaged Reynolds equations for momentum and the thermal energy equation are solved together with the transport equations for the kinetic energy of turbulence k and its rate of dissipation ϵ. Buoyancy effects on both the mean motion and turbulence are considered. The turbulent momentum and thermal diffusivity at the bottom boundary are based on the Monin-Abukhov length scale L for the given buoyancy flux SIG.

The set of equations is solved in the primitive form by an explicit numerical method on a staggered mesh. Marching through time the solution is proceeded until a steady state solution is obtained. Pressure iterations are carried out at each computational step to satisfy the mass conservation equation.

The model results are compared with experimental values of a physical model for fire plumes. The model also predicts the three components of wind mean velocity pressure, potential temperature, density deficit as well as turbulence kinetic energy and its rate of dissipation at different locations of the flow domain. The effects of surrounding environmental circulation are also predicted for different values of bottom heat flux $\dot{Q}''$.

INTRODUCTION

In the last two decades increased efforts have been made to gain an understanding of free burning fire in an attempt to achieve more effective methods for detection and control.

One of many individual problems which must be addressed is to obtain complete understanding and prediction of wind flow pattern around fire areas at different values of buoyancy flux and surrounding circulation.

---

* Mechanical Engineering Department, Faculty of Engineering at Shoubra, Cairo, Egypt.

Such a fire creates a huge central convective plume, which rises to large heights, and very strong radially-inward wind flow in the atmospheric surface layer. The low level inflow increases mixing and provides fresh air to the burning area and inhibits the outward radial spread of the fire.

Moreover, and beyond the scope of the present work, are the large firestorms produced by nuclear bombing. Cotton [1] showed that such storms would have profound effects on the Earth's atmosphere. Smoke particles injected into the stratosphere could widely spread, blocking solar radiation and thus causing a considerable drop in temperature at the Earth's surface and a "Nuclear Winter" would threaten life over a vast area.

Integral theory of free buoyant plumes was developed by Morten, Taylor and Turner [2]. Latter, calculations by Smith, Morten and Lesslie [3] indicated that the buoyancy generated pressure forces control the low level entrainments of ambient air into the fire. The integral theory of buoyant plumes of Morten et al. [2] was modified by Carrier, Fendell and Feldman [4] to study convective column of fire including the pressure gradients effects. No effects of surface layer not those of ambient circulation were considered.

The object of the present work is to consider a numerical model for wind flows above fire areas that includes the effects of buoyancy, pressure gradients, surface layer and ambient circulation.

THE BASIC EQUATIONS

The basic equations are considered in cylindrical coordinates for axisymmetric flow. Reynolds equation of motion given by Hinze [5] (p. 28) for an incompressible flow. The assumption of incompressibility is also used everywhere in the equations except in the body force term where the Boussinesq approximation is considered. The gradient model is assumed for the Reynolds stresses. Rotational effects of Earth are neglected because of the relatively small horizontal extent of the fire considered (few hundreds meters). The flow domain is shown in Figs. 1 and 2. They show a cylindrical domain of radius Ro, height H and concentric fire area of radius Rf at its bottom. Appropriate Equations for the analysis are as follows:

(i) **Mass Conservation:**

$$\frac{1}{r}\frac{\partial}{\partial r}(Ur) + \frac{\partial W}{\partial z} = 0 \ , \qquad (1)$$

(ii) **Radial Momentum:**

$$\frac{\partial U}{\partial t} + \frac{1}{r}\frac{\partial (U^2 r)}{\partial r} + \frac{\partial (UW)}{\partial z} - \frac{V^2}{r} = -\frac{1}{\rho}\frac{\partial p}{\partial r} + \frac{1}{\rho r}\frac{\partial}{\partial r}(2r\mu_{eff}\frac{\partial U}{\partial r})$$

$$+ \frac{\partial}{\rho \partial z}[\mu_{eff}(\frac{\partial U}{\partial z} + \frac{\partial W}{\partial r})] - 2\frac{\mu_{eff}}{\rho}(\frac{U}{r^2}) \ , \qquad (2)$$

(iii) **Tangential Momentum:**

$$\frac{\partial V}{\partial t} + \frac{1}{r}\frac{\partial}{\partial r}(rUV) + \frac{\partial}{\partial z}(WV) + \frac{UV}{r} =$$

$$\frac{1}{\rho}\frac{\partial}{\partial z}(\mu_{eff}\frac{\partial V}{\partial z}) + \frac{1}{\rho r^2}\frac{\partial}{\partial r}[r^3\mu_{eff}\frac{\partial (V/r)}{\partial r}] \qquad (3)$$

6

(iv) Axial Momentum:

$$\frac{\partial W}{\partial t} + \frac{1}{r}\frac{\partial (WrU)}{\partial r} + \frac{\partial (W^2)}{\partial z} = -\frac{1}{\rho}\frac{\partial p}{\partial z} + \frac{1}{\rho}\frac{\partial}{\partial z}\left(2\mu_{eff}\frac{\partial W}{\partial z}\right)$$

$$+ \frac{1}{r\rho}\frac{\partial}{\partial r}\left[r\mu_{eff}\left(\frac{\partial U}{\partial z} + \frac{\partial W}{\partial r}\right)\right] - g\beta(T - T_o) \quad . \tag{4}$$

(v) Turbulence Transport Equations:

Following Jones and Launder [6] the tubulent viscosity U_T is considered to be determined uniquely by local values of density ρ , turbulence kinetic energy per unit mass k and its rate of dissipation ϵ. Thus for dimensional homogeniety;

$$\mu_T \equiv C_\mu \rho \frac{k^2}{\varepsilon} \quad , \tag{5}$$

and the effective viscosity μ_{eff} is given by:

$$\mu_{eff} = C_\mu \frac{\rho k^2}{\varepsilon} + \mu_{laminar}$$

The values of k and ϵ are determined from the solution of their transport equations. The stability effects on the turbulent kinetic energy due to buoyancy at the fire area and that due to swirl (for runs with surrounding circulation) are both included in the transport equations for kinetic energy of turbulence k and its rate of dissipation ϵ.

Transport Equation for Kinetic Energy of Turbulence:

$$\rho\left[\frac{\partial k}{\partial t} + \frac{\partial}{r\partial r}(Ukr) + \frac{\partial}{\partial z}(Wk)\right] =$$

$$\mu_T\{2[(\frac{\partial U}{\partial r})^2 + (\frac{\partial W}{\partial z})^2 + (\frac{U}{r})^2] + (\frac{\partial U}{\partial z} + \frac{\partial W}{\partial r})^2 + (\frac{\partial V}{\partial z})^2 + r^2(\frac{\partial (V/r)}{\partial r})^2\}$$

$$+ g\beta\frac{\mu_T}{\sigma_h}(\frac{\partial T}{\partial z}) + \frac{\partial}{\partial z}[(\mu + \frac{\mu_T}{\sigma_k})(\frac{\partial k}{\partial z})] + \frac{\partial}{r\partial r}[(\mu + \frac{\mu_T}{\sigma_k})\frac{r\partial k}{\partial r}] - \rho\varepsilon \tag{6}$$

Transport Equation for Turbulence Dissipation Rate:

$$\rho\left[\frac{\partial \varepsilon}{\partial t} + \frac{1}{r}\frac{\partial}{\partial r}(U\varepsilon r) + \frac{\partial}{\partial z}(W\varepsilon)\right] =$$

$$\frac{\varepsilon}{k}C_1 P_s + \frac{\partial}{\partial z}\left[(\mu + \frac{\mu_T}{\sigma_\varepsilon})\frac{\partial \varepsilon}{\partial z}\right] + \frac{1\partial}{r\partial r}\left[r(\mu + \frac{\mu_T}{\sigma_\varepsilon})\frac{\partial \varepsilon}{\partial r}\right] - C_2\rho\frac{\varepsilon^2}{k} \tag{7}$$

The Prandtl numbers considered for turbulence kinetic energy and dissipation rate are $\sigma_k = 1$, $\sigma_\epsilon = 1.3$ respectively. The coefficient C_1 is constant and equal to 1.44. The coefficients C and C_μ are also constants for flows with high values of turbulence Reynolds number R_t ($R_t = \rho k^2/\mu\epsilon$). Close to the ground, in the converging zone, C_2 and C_μ are assumed to be functionsof R_t. The experssions given by Launder and Spalding [7] are used,

$$C_2 = 1.92\ (1 - 0.3\ EXP\ (-R_t^2)) \tag{8}$$

$$C_\mu = 0.09\ EXP\ (-3.4/(1 + R_t/50)^2) \tag{9}$$

Ps in equation 7 is the production term. It includes both mechanical production of turbulence energy by the working of mean flow on the turbulent Reynolds stresses and buoyancy production. The temperature field is obtained from the solution of the thermal energy equation where the dissipation of turbulence kinetic energy into heat by viscous action is considered.

(vi) Thermal Energy Equation:

$$\rho\ [\frac{\partial T}{\partial t} + \frac{1}{r}\frac{\partial}{\partial r}\ (TUr) + \frac{\partial}{\partial z}\ (TW)] - \frac{1}{C_p}\frac{DP}{DT} =$$

$$[\frac{1}{r}\frac{\partial}{\partial r}\ (\frac{\mu_{eff}}{\sigma_h}\ r\ \frac{\partial T}{\partial r}) + \frac{\partial}{\partial z}\ (\frac{\mu_{eff}}{\sigma_h}\frac{\partial T}{\partial z})] + \mu\ \{2[(\frac{\partial U}{\partial r})^2 + (\frac{U}{r})^2 + (\frac{\partial W}{\partial z})^2]$$

$$+ [(\frac{\partial V}{\partial z})^2 + (\frac{\partial W}{\partial r} + \frac{\partial U}{\partial z})^2 + (r\frac{\partial}{\partial r}\ (V/r))^2]\}\ /C_p + \rho\varepsilon/C_p \tag{10}$$

For environmental applications it is convenient to introduce the potential temperature Θ, which is defined as the temperature that would result if the air were brought isentropically to a reference pressure P_{ref};

$$\Theta = T\ (P_{ref}/P)^{(\frac{\gamma-1}{\gamma})}\ ;\ \text{where } \gamma \text{ is the specific heats ratio}$$

Using the potential temperature the pressure derivative term in equation (10) is cancelled and the conservation equation of potential temperature is considered.

Boundary Conditions

The basic equations are solved in the primitive form on the simplified flow domain shown in figure 2. The figure also shows the boundary conditions for all the dependent variables. The configuration is based on both the schematic description of large fire areas by Small and Larson [8] shown in Fig. 1 and the laboratory model for fire plume by Poreh and others [9]. The boundary conditions are as follows:

(1) Bottom Boundary at z = o

$U = V = W = O$ at any radius

$\Theta = T_o$ at $Rf < r \leqslant Ro$

$-\frac{\partial \theta}{\partial z} = \frac{SIG\ T_o}{g\ K_h}$ at $O \leqslant r < Rf$

Where SIG is the the buoyancy flux in m^2/s^3 and defined by;

$$SIG = g\,\dot{Q}''/(T_o \rho C_p).$$

T_o is the reference potential temperature outside the fire and K_h is the turbulent thermal diffusivity at the fire area. Its magnitude is an important factor in determining the potential temperature gradient at the bottom of the domain, and is calculated using the profile for the thermally unstable surface layer, given by Turnner [10] as follows:

$$K_h = k_1 u_*^3 z/\Phi_h \quad , \ \Phi_h \text{ is the dimensionless heat flux function}$$

$$\Phi_h = 0.74\,(1 - 9\,z/L)^{-1/2}$$

Where u_* is the shear velocity, k_1 is von Karman constant with value of 0.4 and L is the Monin-Obukhov length scale; a scalling parameter which is negative for the present unstable condition (heating from below) and is given by;

$$L = -u_*^3 / (k_1 SIG)$$

z is the axial coordinate for the first nodal point where the above bottom boundary condition is applied. Similarly the turbulent eddy diffusivity at the first nodal point is calculated using the dimensionless wind shear function Φ_m

$$\Phi_m = (1 - 15\,z/L)^{-1/4}$$

Values of the dissipation ϵ at the first nodal point above the ground are based on measurements by Wyngaard and Cote [11] in an unstable atmosphere;

$$\epsilon = \frac{u_*}{k_1 z}\,(1 + 0.5\,|(z/L)|^{2/3})^{1.5}$$

The kinetic energy of turbulence at the first nodal point next to the bottom boundary is based on the measurements reported by Patel et al [12] near the ground and away from the laminar sublayer. The rest of boundary conditions are shown in figure 2. For large negative values of (Z/L), the limiting values of Φ_h and Φ_m of free convection are taken from the observations of Charnock [13].

Numerical Solution

The flow variables are defined on a staggered mesh. For the cell ij, the radial velocity $U^{i+1/2,j}$ is defined at the center of the right side of the cell and the axial velocity $W^{i,j+1/2}$ is defined at the center of its top. All other flow variables are defined at the cell center. To obtain fine resolution near the ground (combustion zone) and close to the fire center stretched coordinates in both r and z are used.

An explicit time dependent method for the primitive equations is used. The solution is obtained by advancing the flow field variables through a sequence of time steps untill a steady state condition is achieved. The advancement of one step is calculated in two stages. The first is a simple explicit calculation of all the variables, (pressure gradient term is excluded from radial and axial momentum equations). The second stage is an iterative correction of the pressure and convective velocity components U and W to satisfy equation (1) of mass conservation. The donor cell treatment (a central - upwind hybrid method) of

Amsden and Harlow [14] is used for convective terms of all equations and the central difference method for diffusion terms.

Results

The strongly buoyant flow generated around a large area fire is predicted using an appropriate two-equation turbulence model. To verify the model, the results of dimensionless density deficit are compared with the available experimental values of the physical fire model by Poreh et al. [9] measured near the center of the plume. Figure 3 shows that the present model results at $r/R_o = 0.135$ compare favourably with experimental values. The discrepancy between experimental and numerical values at smaller radii may be explained that Boussinesq approximation, used in the model is not adequate for large density variations used for the light gas in the physical model.

Figures 4a and 4b show the radial distribution of the dimensionless axial velocity at different heights of the fire plume. The characterstic velocity $(SIG\ Rf)^{(1/3)}$ is used for normalization. The axial velocity has a maximum value near $z/Rf = 0.7$, which corresponds to the height of the pinch point of both experiment and field observations of fire plumes and is shown in Fig. 1.

The figures also show that plume radius, close to combustion zone, is approximately equal to the fire radius Rf. It increases with height and equals about twice the fire radius at a dimensionless height z/Rf of about 1.4. At the top of the computational domain, $z/Rf = 8$ the plume radius is about 4 Rf.

In order to discuss the effects of axisymmetric environmental circulation Γ on the fire convective plume, The swirl ratio S is defined as;

$$S = (\Gamma R_o)/(2Q)$$

where Q is the total volume flow rate through the plume. Figure 5 shows the radial distribution of dimensionless axial velocity for two different values of swirl ratio S, and same buoyancy flux SIG. It shows a considerable increase fire updraft with the increase of swirl ratio. Figure 6 shows the profiles of dimensionless radial component of velocity (entrainment velocity). The results show that the dimensionless entrainment velocity near the ground increases from 0.17 at $S = 0.18$ to 0.23 at $S = 0.7$, for a given value of buoyancy flux. The inward radial pressure gradient created by the upper environmental circulation causes an increase of both entrainment velocity at the surface layer zone and updraft velocity at the convective plume. Figure 7 shows the dimensionless increase of potential temperature for different values of swirl and the same value of buoyancy flux SIG. An increase of S causes an increase of the temperature difference. Accordingly the convective heat from the combustion zone increases with the increase of the swirl ratio S.

References

[1] Cotton, W.R. "Atmospheric Convection and Nuclear Winter, "American Scientist, Vol. 73, No. 3, May-June, 1985.

[2] Morton, B.R., Taylor, G.I. and Turner, J.S. "Turbulent Gravitational Convection from aintained and Instantaneous Source", Proceedings of the Royal Society of London, A-23A, pp. 1-23.

[3] Smith, R.K., Morton, B.R. and Leslie, L.M. "The Role of Dynamic Pressure in generating Fire Winds," Journal of Fluid Mechanics, Vol. 68, pp. 1-19. (1975).
[4] Carrier, G.F., Fendel, F.E. and Feldman, P.S. "Firestorms," Journal of Heat Transfer, ASME, Vol. 107, No. 1, pp. 19-27. (1985).
[5] Hinze, J.O. "Turbulence," McGraw-Hill Book Company, 790 p. (1975).
[6] Jones, W.P. and Launder, B.E. "The Prediction of Laminarization with Two-Equation Model of Turbulence," International Journal of Heat and Mass Transfer, Vol. 15, pp. 301-314. (1972).
[7] Launder, B.E. and Spalding, B.D. "The Numerical Computation of Turbulent Flows," Computer methods in applied Mechanics and Engineering, Vol. 3, pp. 269-289. (1974).
[8] Small R.D. and Larson D.A. "Velocity Fields Generated by Large Fires," 26th Israel Annual Conference on Aviation and Astronautics, February. (1984).
[9] Poreh, M., Stout., J.E., Cermak, J.E. and Peterka, J.A. "Physical Simulation of Flow Induced by Large Fires.," Colorado State University Report CER 84-85 MP. (1985).
[10] Turner, J.S. "Buoyancy Effects in Fluids," Cambridge University Press, London, 368 p. (1979).
[11] Wyngaard, J.C. and Cote, O.R. "The Budgets of Turbulent Kinetic Energy and Temperature Variance in the Atmospheric Surface Layer," Journal of Atmospheric Sciences, Vol. , No. 1, pp. 188-197. (1971).
[12] Patel, V.C., Rodi, W. and Scheuerer G. "Turbulence Models for Near Wall and low Reynolds Number Flows: A Review, "Journal of American Institute of Aeronautics and Astronautics, Vol. 23, No. 9, pp. 1308-1319. (1985).
[13] Charnock, H. "Flux Gradient Relations Near the Ground in Unstable Conditions," Quarterly Journal of Royal Meterological Society, Vol. 93 p. 133, (1967).
[14] Amsden, A.A. and Harlow, F.H. "The SMAC Method," Los Almos Scientific Laboratory Report No. LA 3470 (1970).

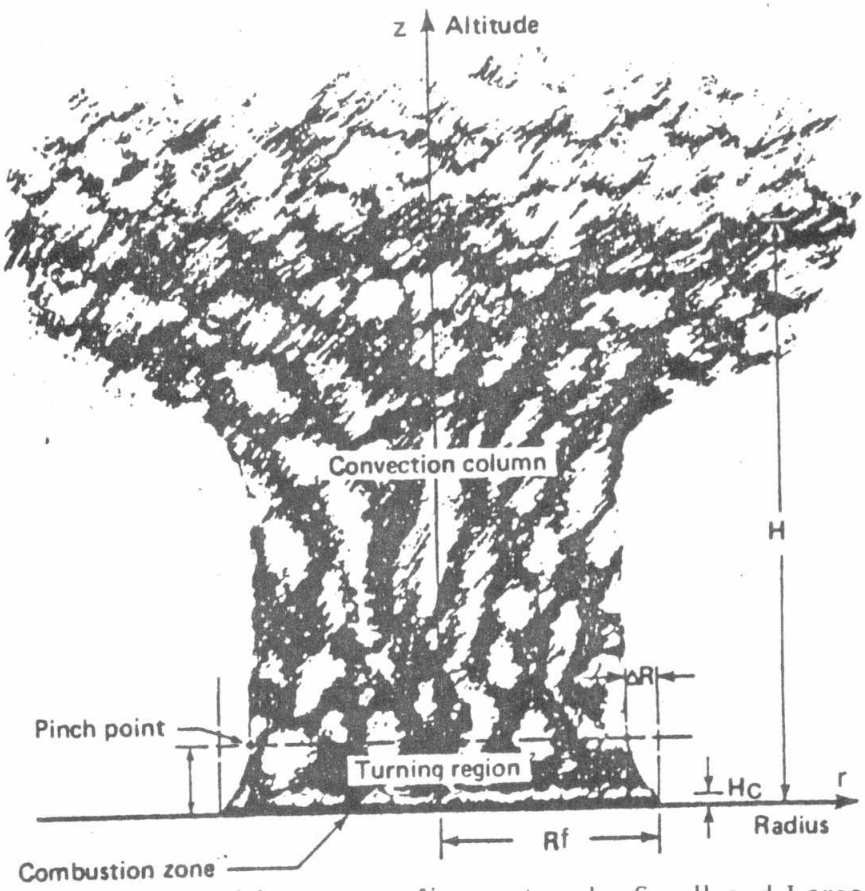

Fig. 1. Schematic of large-area-fire system by Small and Larson [8].

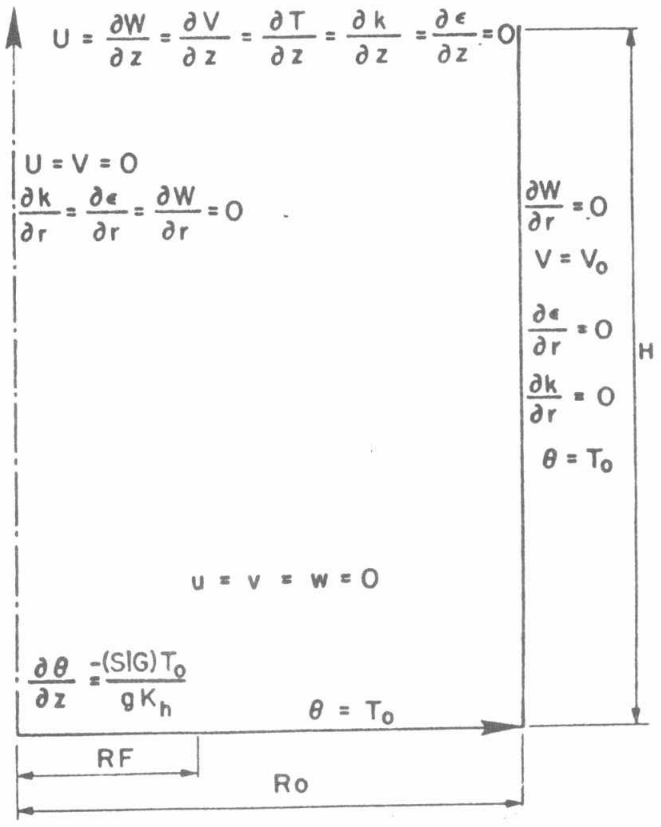

Fig. 2. The computational domain for the fire model

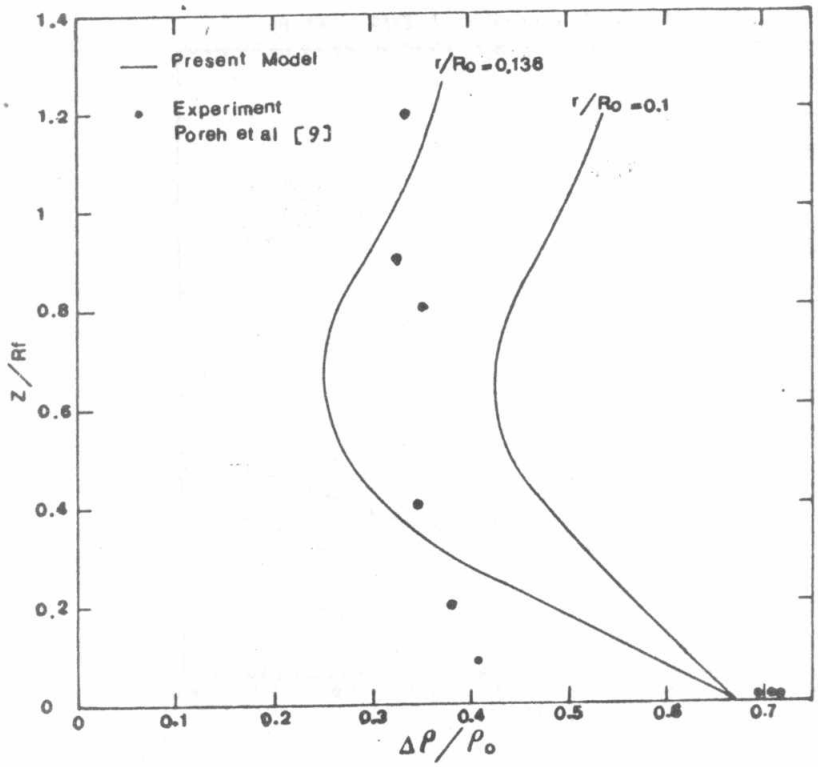

Fig. 3. Comparison between experimental and numerical results of the dimensionless density deficit, SIG = 0.335 m^2/S^3, S = o.

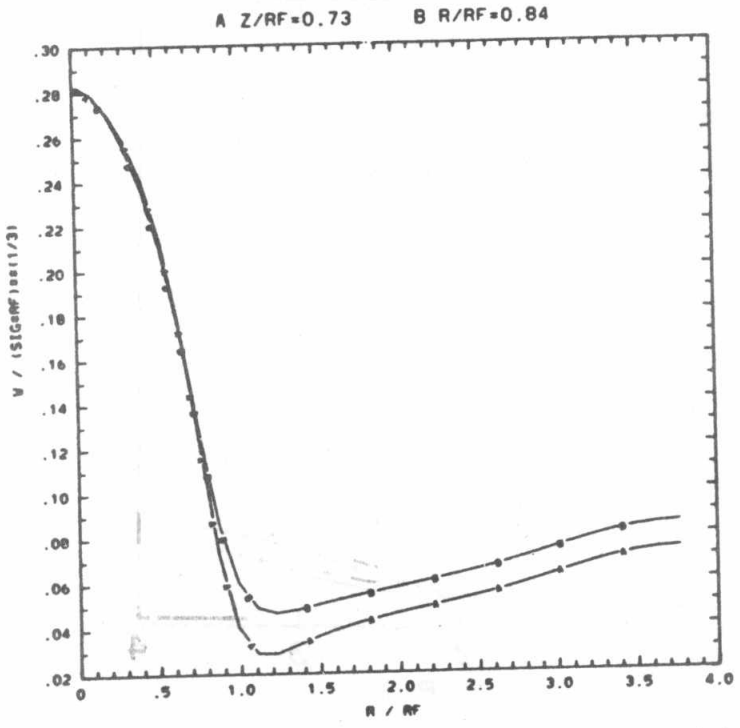

Fig. 4a. Radial distributions of dimensionless axial velocity, SIG = 2.1 m^2/S^3 and S = 0.4.

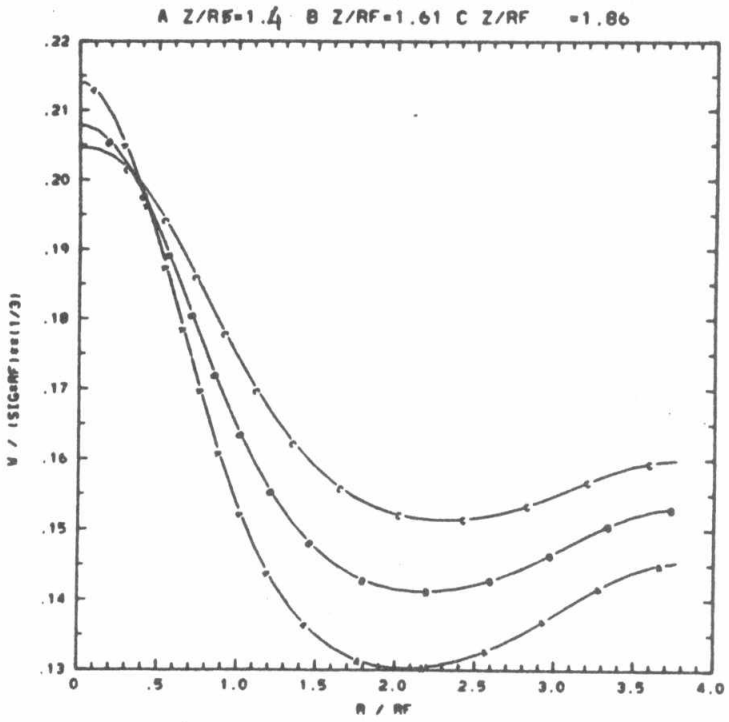

Fig. 4b. Radial distributions of dimensionless axial velocity SIG = 2.1 m^2/S^3 and S = 0.4

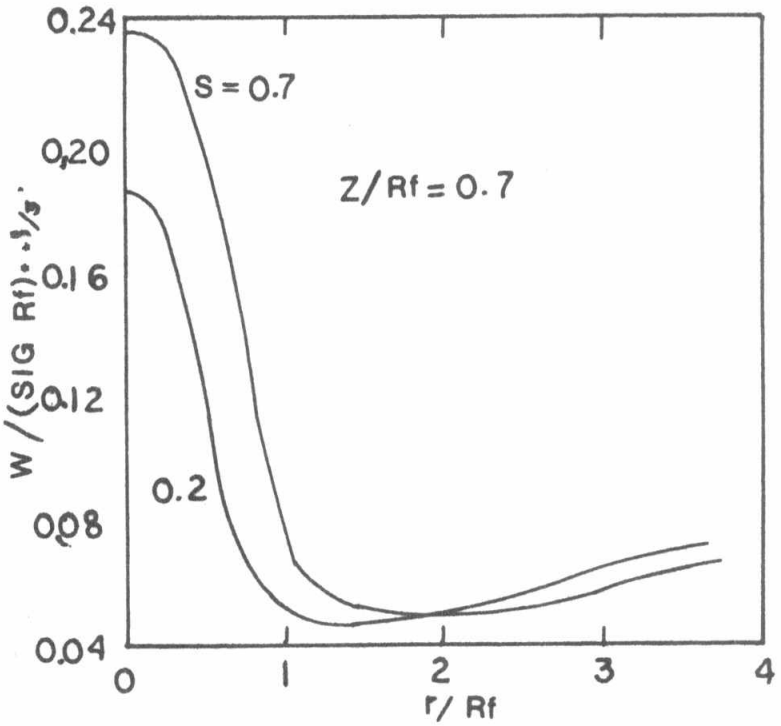

Fig. 5. Effect of the swirl rato S on axial velocity SIG = 1 m^2/S^3

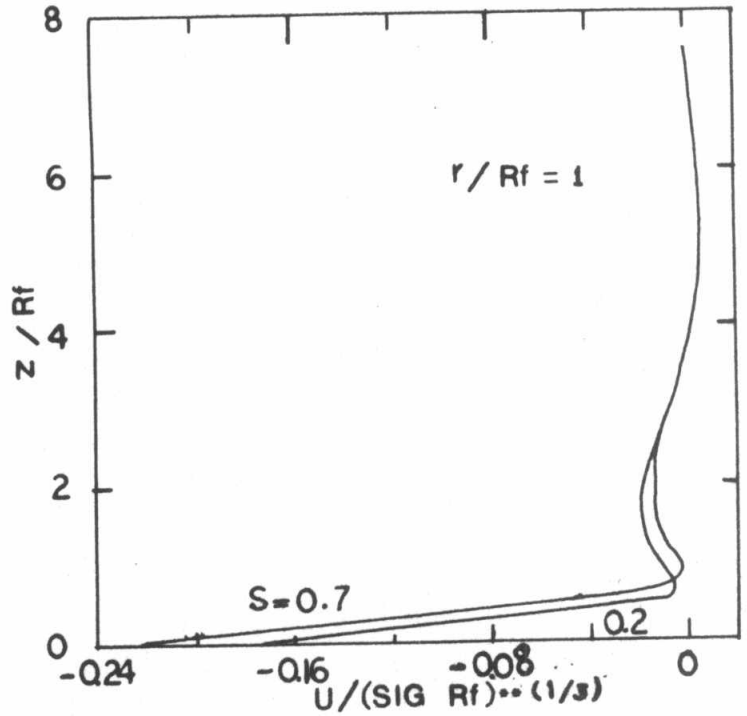

Fig. 6. Effect of the swirl ratio S on the dimensionless radial velocity profile near the fire radius R_f, SIG = 1 m^2/S^3.

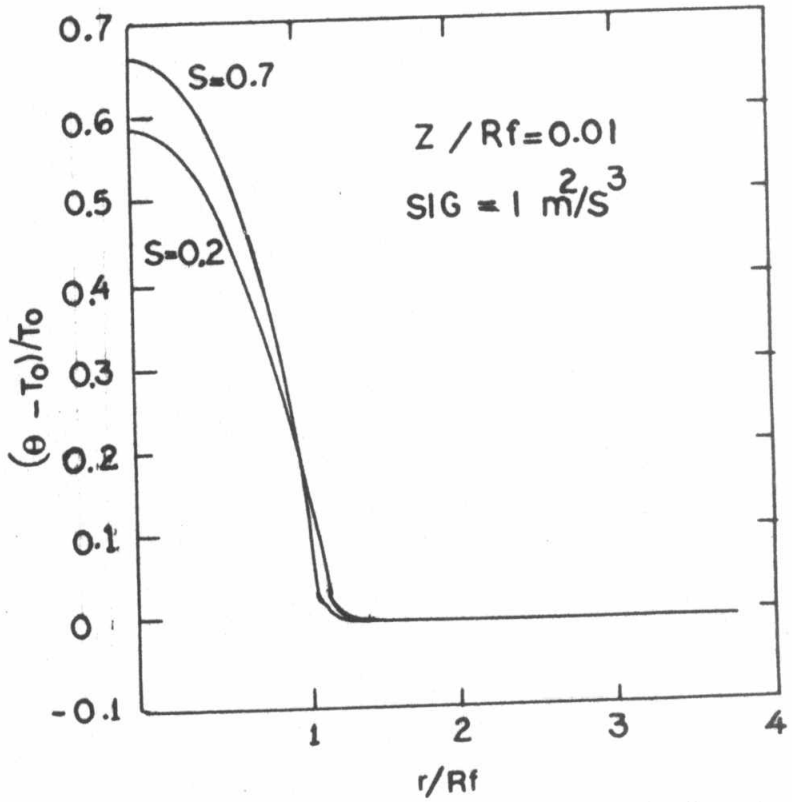

Fig. 7. Effect of swirl ratio S on the dimensionless increase of potential temperature SIG = 1 m^2/S^3.